

Steady two-dimensional thermal convection in a vertical porous slot with spatially periodic boundary imperfections

D. S. RILEY

School of Mathematics, University of Bristol, University Walk, Bristol BS8 1TW, U.K.

(Received 1 October 1987 and in final form 19 May 1988)

Abstract—Steady, two-dimensional, thermal convection in a vertical slot filled with a saturated porous medium is considered when the sidewalls are held at different constant temperatures and are misaligned, i.e. surface undulations exist. The spatial nonuniformities at the two walls are assumed to have small amplitudes and common (arbitrary) wave number. Attention is focused on the core flow, which is assumed to lie in the conductive regime. In the absence of nonuniformities this flow is unconditionally stable, consequently the actual flow is purely baroclinic and there is no thermoconvective instability. Nusselt number results are presented and it is found that out-of-phase imperfections enhance the heat transfer significantly.

INTRODUCTION

THE 'DOUBLE-glazing' problem of free convection of a Darcy-Boussinesq fluid saturating a porous cavity with vertical walls maintained at two different temperatures and horizontal walls adiabatic has received considerable attention in the recent past [1-19]. This work has been stimulated by applications ranging from building science to geophysics. Building science and thermal engineering applications were first motivated by the fact that an appreciable insulating effect may be derived from the placing of porous material in the gap between cavity walls, and in multishield structures between the pressure vessel and the reactor in nuclear power installations. The geophysical applications include modelling the spreading of pollutants (such as radionuclides), geothermal-energy reservoirs and convection in the Earth's mantle.

The theoretical work may be conveniently classified in (Ra, L) space, where Ra is the Rayleigh number based on the height h of the cavity and L is the aspect ratio, l/h where l is the length of the cavity. Blythe *et al.* [17] did this, by considering various distinguished limits that arise, and by setting previous asymptotic analyses in their proper context. In particular, they identified five regions of the parameter space.

(i) Fixed $Ra/L < 10$, $L \rightarrow \infty$ —the Hadley regime. This shallow cavity problem was analysed by Walker and Homsy [9] and by Bejan and Tien [10]. Away from end zones near the vertical walls, there is weak horizontal flow driven by a constant horizontal temperature gradient. This central core flow is turned in the end zones wherein diffusion dominates.

(ii) $10L < Ra < 30L^2$, $L \rightarrow \infty$ —the intermediate regime. This is similar in structure to the Hadley regime in that the core equations are exactly the same

but the flow is much stronger, and convection balances diffusion in the end zone [19].

(iii) $30L^2 < Ra < 10^4 L^2$, $L \rightarrow \infty$ —the merged regime. In this regime, the core flow is stronger with the consequence that convection now balances with vertical diffusion. Convection also balances diffusion in the end zone [17].

(iv) $Ra > 6.81L^{-2}$ —the vertical boundary layer regime. Here the dominant mode of heat transfer across the cavity is convection, with horizontal diffusion important only in thin layers next to the vertical walls.

(v) $Ra > 10^4 L^2$ —this condition, which is particularly severe for shallow cavities with $L \gg 1$, marks the appearance of thin horizontal boundary layers.

The 'boundary-layer problem', where conditions (iv) and (v) are both satisfied, was first analysed by Weber [7], who neglected the effects of the horizontal boundary layers. Walker and Homsy [9] attempted to extend the analysis to include these layers and then Blythe *et al.* [15] and Daniels *et al.* [16] gave a first-order description of the entire flow field, including the corner interaction regions (see also Simpkins and Blythe [13] and Bejan [12]). The 'conduction problem', where (iv) is not satisfied and the vertical layers fill the slot, has been partially analysed by Gill [1]. As far as the present author is aware a complete description has not been found for this case, which can easily arise for tall slots, nor indeed have descriptions been given for the other distinguished limits that arise for tall slots.

A less comprehensive classification was offered by Prasad and Kulacki [18], who compared asymptotic results with numerical results obtained by themselves and by others cited in their paper. Prasad and Kulacki classify the flow regimes into three categories.

NOMENCLATURE

a_r, a_l	boundary amplitudes	Greek symbols	
A	Rayleigh number based upon length	β	phase difference in boundary imperfections
g_r, g_l	boundary-shape functions	γ	coefficient of cubical expansion
h	semi-height of cavity	δ	boundary amplitude scale
H	aspect ratio (height/length)	η	transformed horizontal coordinate
k	wave number of boundary imperfections	θ	dimensionless temperature
K	permeability of the porous medium	κ	thermal diffusivity
l	mean semi-length of cavity	λ	thermal conductivity
L	aspect ratio (length/height)	μ	coefficient of viscosity
\underline{L}_1	operator defined by equation (7)	ν	coefficient of kinematic viscosity
\overline{Nu}	mean Nusselt number	ξ	transformed vertical coordinate
Q	through-flow	ρ	density
Ra	Rayleigh number based on height	ψ	dimensionless stream-function.
s_1, s_2	defined by equations (8)	Subscripts	
ΔT	half the applied temperature difference	f	fluid
x, y	dimensionless Cartesian coordinates.	m	saturated porous medium.

(i) The conduction regime in which there is little or no vertical stratification of the core and the flow is moderate; this situation is obtained when either (a) $Ra \rightarrow 0$, L finite or (b) finite $Ra \times L$, $L \rightarrow 0$ or ∞ .

(ii) The asymptotic regime in which there is significant stratification of the core and convective heat transfer; this situation is obtained when

$$Ra > (4.65 \pm 0.15)L^{-1.73}, \quad L < 0.5$$

$$Ra > 33.5 - 115.7/L + 218.2/L^2 - 198.4/L^3 + 88.1/L^4 - 15.0/L^5, \quad 0.5 < L < 5$$

and

$$Ra > (3.9 \pm 0.2)L^{0.95}, \quad L > 5.$$

This regime seems to encompass both the Hadley and intermediate regimes above.

(iii) The boundary layer regime in which there are boundary layers formed and the dominant mode of heat transfer across the cavity is convection; for tall cavities this regime exists when

$$Ra > (37.2 \pm 0.8)/L^{1.85}, \quad L < 0.5.$$

Prasad and Kulacki also introduce a 'pseudo boundary-layer' regime which exists for shallow cavities and seems to be equivalent to the merged layer regime above. It should be stressed that the criteria used by Prasad and Kulacki are rather subjective and so it is not terribly clear how the two categories are related.

The concern of the present study is with the conductive regime in a tall slot and it is assumed that $A = Ra \times L = O(1)$ as $L \rightarrow 0$. In the absence of boundary imperfections, the structure of the flow field is similar to that in the analogous Newtonian fluid problem considered by Daniels [20]: away from the

horizontal boundaries there is a horizontally stratified vertical flow with a quadratic velocity profile corresponding to upward motion in the hotter half of the slot and downward motion in the cooler half. The vertical two-way flow is turned in roughly square end zones near the horizontal boundaries. The flow in these zones is nonlinear, unless $A \ll 1$. It is the aim of this paper to elucidate the effects of boundary imperfections on the flow and heat transfer in the core region of the slot. The end zones, in general, require a numerical solution of the full non-linear Darcy-Boussinesq equation and will be considered in a later study.

This paper presents the first steps in generalizing the 'cavity-wall' problem to the more realistic situation of non-planar boundaries. Non-planar boundaries are certainly the rule rather than the exception in insulation problems, and it is well known that a common difficulty encountered in experimental studies of cavity flows is that of obtaining walls of perfect alignment and length. In essence the study concentrates on the effects of single modes from the Fourier decomposition of the general boundary disposition, and focuses upon the flow in the core region.

FORMULATION

The problem to be considered is that of the steady motion and heat transfer which occur when a vertical slot filled with a fluid-saturated porous medium is contained between two slightly misaligned, impermeable sidewall boundaries, the surfaces of which are maintained at constant temperatures $\pm \Delta T$, respectively, where $\Delta T > 0$. The horizontal bounding sur-

faces are taken to be perfectly level and adiabatic. The mean disposition of the slot is vertical with mean length $2l$ and height $2h$ (Fig. 1).

Subject to the Darcy–Boussinesq approximations, the governing non-dimensional equations are

$$\nabla^2 \psi = A \frac{\partial \theta}{\partial y} \tag{1}$$

$$\nabla^2 \theta = \frac{\partial(\theta, \psi)}{\partial(x, y)} \tag{2}$$

where ψ is the stream-function, θ the temperature and x, y are dimensionless Cartesian coordinates based at the centre of the slot in the absence of boundary imperfections. Here A is the Darcy–Rayleigh number (based upon length) defined by

$$A = (g\gamma\Delta TKl)/(\nu\kappa) \tag{3}$$

where K is the permeability, γ the coefficient of cubical expansion of the saturating fluid, g the acceleration due to gravity and ν, κ the coefficients of kinematic viscosity and thermal diffusivity, respectively. Variables have been non-dimensionalized using length, velocity, pressure and temperature scales given by

$$l, \kappa/l, (\kappa\mu)/K, \text{ and } \Delta T$$

where μ is the coefficient of viscosity and $\kappa = \lambda_m/(\rho c)_f$. Here λ_m, ρ and c denote respectively thermal conductivity, density and specific heat; subscripts f and m signify values for the fluid and saturated medium, respectively. Furthermore ∇^2 denotes the two-dimensional Laplacian in x and y and

$$\frac{\partial(\theta, \psi)}{\partial(x, y)} = \frac{\partial\theta}{\partial x} \frac{\partial\psi}{\partial y} - \frac{\partial\theta}{\partial y} \frac{\partial\psi}{\partial x}$$

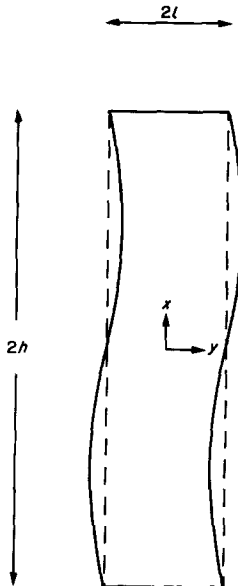


FIG. 1. Schematic of the cavity cross-section.

The lateral surfaces are defined by

$$y = \{-1 - \delta g_l(x)\} \quad \text{and} \quad y = \{1 + \delta g_r(x)\}$$

where the scale of the boundary imperfection $\delta \ll 1$, and the g 's, which are boundary-shape functions, are arbitrary. In fact it is assumed that the shape functions are Fourier analysable and a single mode is focused upon, so that

$$g_l(x) = a_l \cos(kx + \beta) \quad \text{and} \quad g_r(x) = a_r \cos(kx - \beta)$$

where the a 's are amplitude measures of, and 2β is the phase difference between, the respective spatial variations; k is their common wave number.

The boundary conditions needed to complete the specification of the problem are

$$\psi = 0, \theta = -1 \quad (\text{right-hand boundary: } y = 1 + \delta g_r(x))$$

$$\psi = 0, \theta = 1 \quad (\text{left-hand boundary: } y = -1 - \delta g_l(x)).$$

Results will also be presented for the case where there is a vertical through-flow, in which case the condition on ψ at the right-hand boundary becomes

$$\psi = Q.$$

ANALYSIS

The flow regimes are characterized by the relative sizes of the aspect ratio, $H = h/l$, the Rayleigh number, A , and the scale, δ . The one of present concern is where A and $\delta (\ll 1)$ are of $O(1)$ as $H \rightarrow \infty$. In this case, the flow splits naturally into two regions: (i) the core region, where the flow is purely baroclinic and (ii) the end zones, where the flow direction is reversed. In (i), which is the focus of this paper

$$y, \psi, \theta = O(1) \quad \text{and} \quad x = O(H).$$

The case $\delta = 0$ corresponds to flow in a porous vertical slab, which has previously been considered by Gill [1]. He showed that fully developed counterflow ($Q = 0$), with linear velocity and temperature profiles across the slab, is unconditionally stable to infinitesimal disturbances. The inclusion of through-flow (Q non-zero) does not alter this result, since it can be easily eliminated from the problem by a Galilean transformation. This special case has an exact 'conduction' solution

$$\left. \begin{aligned} \theta &= -y \\ \psi &= A(1-y^2)/2 + Q(1+y)/2 \end{aligned} \right\} \tag{4}$$

and is valid in the core region where $-H < x < H$ and $-1 \leq y \leq 1$.

For $\delta \neq 0$, it is convenient to introduce new variables which straighten out the slot

$$\xi = x, \quad \eta = \frac{2y + \delta[g_l(x) - g_r(x)]}{2 + \delta[g_l(x) + g_r(x)]} \tag{5}$$

The governing equations become

$$\left. \begin{aligned} L_1\psi &= 2s_1 A \partial\theta/\partial\eta \\ L_1\theta + 2s_1 \frac{\partial(\psi, \theta)}{\partial(\xi, \eta)} &= 0 \end{aligned} \right\} \quad (6)$$

where

$$\frac{\partial(\psi, \theta)}{\partial(\xi, \eta)} = \frac{\partial\psi}{\partial\xi} \frac{\partial\theta}{\partial\eta} - \frac{\partial\psi}{\partial\eta} \frac{\partial\theta}{\partial\xi}$$

and

$$\begin{aligned} L_1 &= s_1^2 \frac{\partial^2}{\partial\xi^2} + 2\delta s_1 s_2 \frac{\partial^2}{\partial\eta \partial\xi} + [4 + \delta^2 s_2^2] \frac{\partial^2}{\partial\eta^2} \\ &+ [\delta s_1 \{(1-\eta)g_1'' - (1+\eta)g_1''\} - 2\delta^2 s_2 \{g_1' + g_1'\}] \frac{\partial}{\partial\eta} \end{aligned} \quad (7)$$

with

$$\left. \begin{aligned} s_1 &= 2 + \delta(g_1 + g_1) \\ s_2 &= (1-\eta)g_1' - (1+\eta)g_1' \end{aligned} \right\} \quad (8)$$

One now looks for steady-state solutions and expands

$$\left. \begin{aligned} \psi(\xi, \eta) &= \psi_0(\xi, \eta) + \delta\psi_1(\xi, \eta) + \delta^2\psi_2(\xi, \eta) + \dots \\ \theta(\xi, \eta) &= \theta_0(\xi, \eta) + \delta\theta_1(\xi, \eta) + \delta^2\theta_2(\xi, \eta) + \dots \end{aligned} \right\} \quad (9)$$

The $O(1)$ terms, which are given by equations (4), with y replaced by η , constitute the 'conduction' solution, whilst the $O(\delta)$ terms satisfy

$$\begin{aligned} \nabla^2\psi_1 - A\theta_{1\eta} &= \frac{1}{2}a_l \cos(k\xi + \beta)[k^2(1-\eta)(Q - 2A\eta) - A] \\ &+ \frac{1}{2}a_r \cos(k\xi - \beta)[-k^2(1+\eta)(Q - 2A\eta) - A] \\ \nabla^2\theta_1 - \psi_{1\xi} - \frac{1}{2}(Q - 2A\eta)\theta_{1\xi} &= -\frac{1}{2}a_l \cos(k\xi + \beta)[k^2(1-\eta)] \\ &+ \frac{1}{2}a_r \cos(k\xi - \beta)[k^2(1+\eta)] \end{aligned}$$

with $\psi_1 = \theta_1 = 0$ on $\eta = \pm 1$.

These equations have a solution of the form

$$\begin{aligned} (\psi_1, \theta_1) &= a_l \sin(k\xi + \beta)(f_1, g_1) \\ &+ a_l \cos(k\xi + \beta)(f_2, g_2) + a_r \sin(k\xi - \beta)(f_3, g_3) \\ &+ a_r \cos(k\xi - \beta)(f_4, g_4) \end{aligned} \quad (10)$$

where $\{f_i, g_i: i = 1(1)4\}$ satisfy two linear eighth-order systems of ordinary differential equations, which involve the coupling of the functions with odd and with even subscripts, respectively. The solutions to these systems depend upon the parameters Q, A and k .

The $O(\delta^2)$ terms satisfy equations which have a

solution of the form

$$\begin{aligned} (\psi_2, \theta_2) &= a_l^2 \{ \sin(2k\xi + 2\beta)(f_5, g_5) \\ &+ \cos(2k\xi + 2\beta)(f_6, g_6) + (f_7, g_7) \} \\ &+ a_r^2 \{ \sin(2k\xi - 2\beta)(f_8, g_8) \\ &+ \cos(2k\xi - 2\beta)(f_9, g_9) + (f_{10}, g_{10}) \} \\ &+ a_l a_l \{ \sin(2k\xi)(f_{11}, g_{11}) + \cos(2k\xi)(f_{12}, g_{12}) \} \\ &+ a_l a_l \{ \sin 2\beta(f_{13}, g_{13}) + \cos 2\beta(f_{14}, g_{14}) \} \end{aligned} \quad (11)$$

where $\{f_i, g_i: i = 5(1)14\}$ satisfy a linear, fortieth-order system of ordinary differential equations (which contains independent lower-order sub-systems of equations). This system reduces in special cases such as $a_l = a_r, \beta = 0$, etc. The equations were solved using the NAG routine DO2HAF.

On using $\lambda_m l / \Delta T$ to nondimensionalize the local conductive heat transfer from the right-hand boundary, the mean Nusselt number \bar{Nu} is given by

$$\bar{Nu} = -\frac{k}{2\pi} \int_0^{2\pi/k} \left\{ \frac{1 + [\delta g_1']^2}{1 + \frac{1}{2}\delta[g_1' + g_1]} \right\} \left(\frac{\partial\theta}{\partial\eta} \right)_{\eta=1} d\xi \quad (12)$$

After a little algebra it is found that to $O(\delta^2)$

$$\begin{aligned} \bar{Nu} &= 1 + \frac{\delta^2}{4} \{ a_l^2 [g_2' + \frac{1}{2} - 4g_7'] \\ &+ a_l^2 [2k^2 + g_4' + \frac{1}{2} - 4g_{10}'] \\ &+ a_l a_l [(g_1' - g_3' - 4g_{13}') \sin 2\beta \\ &+ (1 + g_2' + g_4' - 4g_{14}') \cos 2\beta] \}. \end{aligned} \quad (13)$$

RESULTS

The results of the numerical computations are displayed in Fig. 2. In all these plots (i), (ii) and (iii) show $(\psi_0, \theta_0), (\psi_1, \theta_1)$ and (ψ_2, θ_2) , respectively, whilst (iv) displays (ψ, θ) to $O(\delta^2)$. The plots are in pairs with the streamlines on the left and the isotherms on the right; the left-hand wall is the hot one. For illustrative purposes one has taken $\delta = 0.15, a_r = a_l = 1.0$, and $k = 1.5$.

Figures 2(a)–(c) illustrate the development as the Rayleigh number, A , increases in a varicose configuration with zero through-flow ($Q = 0$). The $O(1)$ contributions show no qualitative changes, as expected since the Rayleigh number simply scales ψ_0 , see equations (4). The behaviour of the $O(\delta)$ solutions is qualitatively similar to that found by Wynne [22] in the corresponding Boussinesq fluid problem when the flow is sub-critical. The flow consists of a vertical stack of vortices, each of which displays a tendency to pinch and split as the Rayleigh number increases. It is interesting to note that the inclination of the isotherms switches as the Rayleigh number increases; this is caused by the increased base counter-flow (i.e. the $O(1)$ flow) as A increases. The strength of the counterflow in the resultant flows (vi) increases with A ,

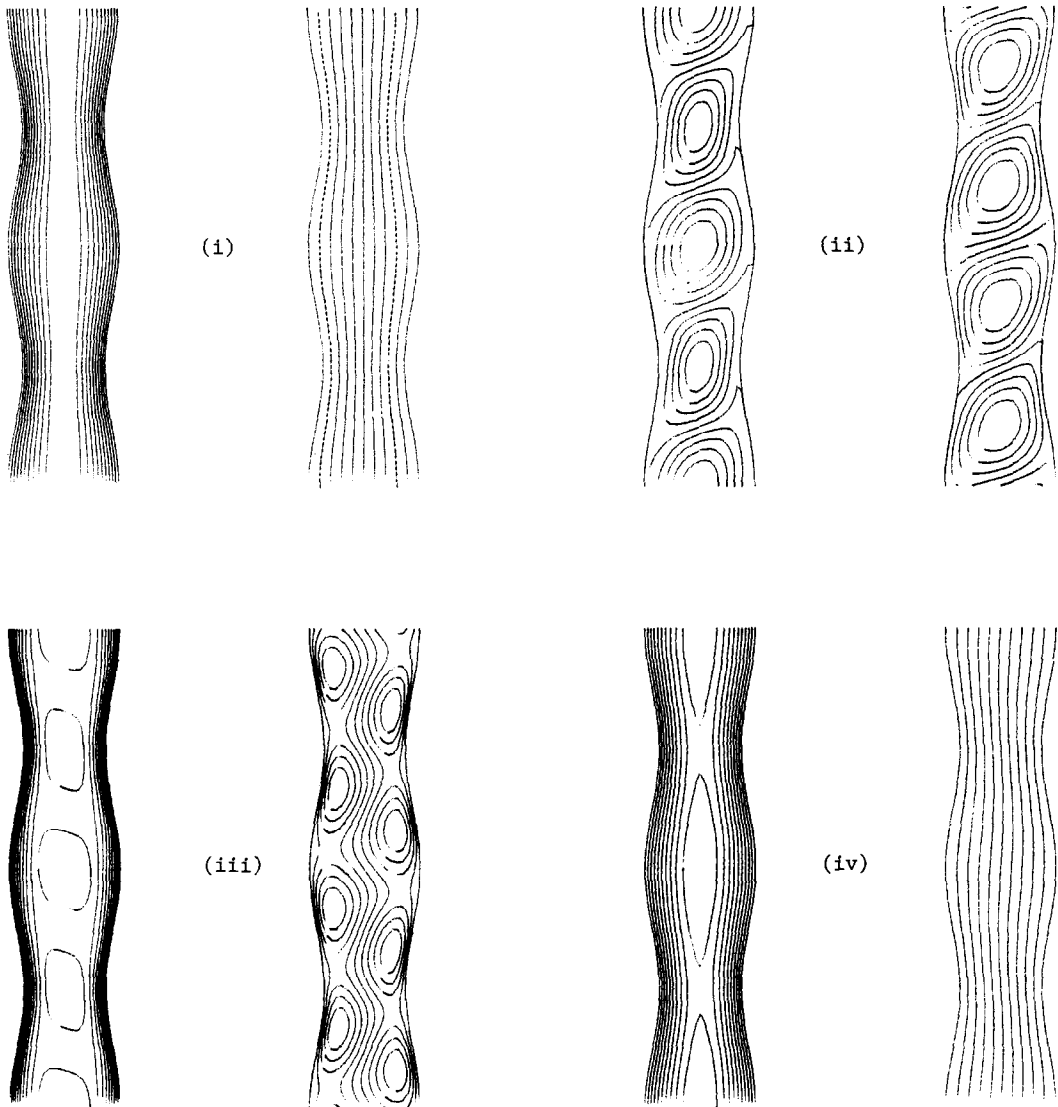


FIG. 2(a). The streamlines (left) and isotherms (right) when $\delta = 0.15$, $a_r = a_l = 1.0$ and $k = 1.5$: (i) $O(1)$, (ii) $O(\delta)$, (iii) $O(\delta^2)$, and (iv) resultant to $O(\delta^2)$. $Q = 0$, $A = 5$, $\beta = 0$.

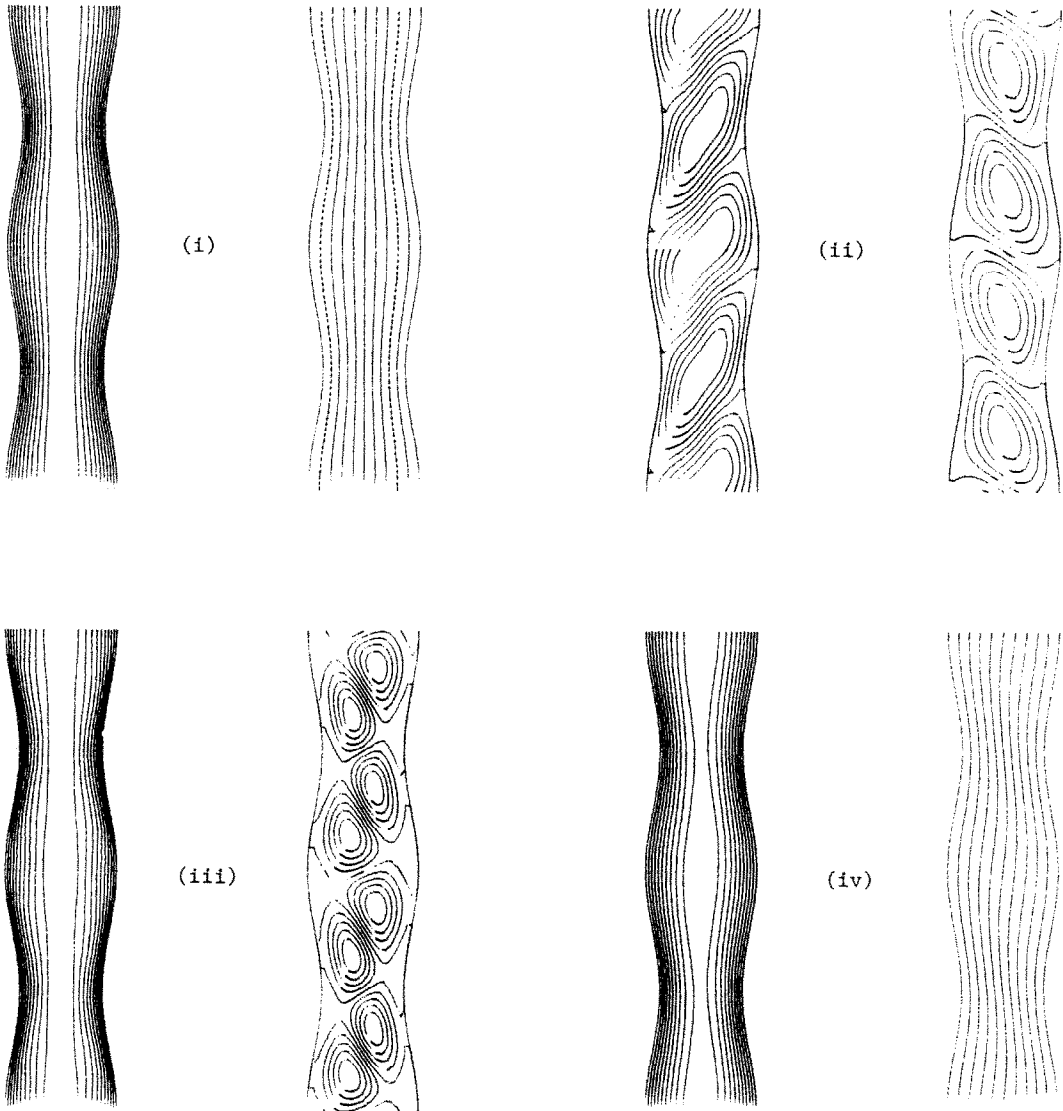


FIG. 2(b). The streamlines (left) and isotherms (right) when $\delta = 0.15$, $a_r = a_l = 1.0$ and $k = 1.5$: (i) $O(1)$, (ii) $O(\delta)$, (iii) $O(\delta^2)$, and (iv) resultant to $O(\delta^2)$. $Q = 0$, $A = 20$, $\beta = 0$.

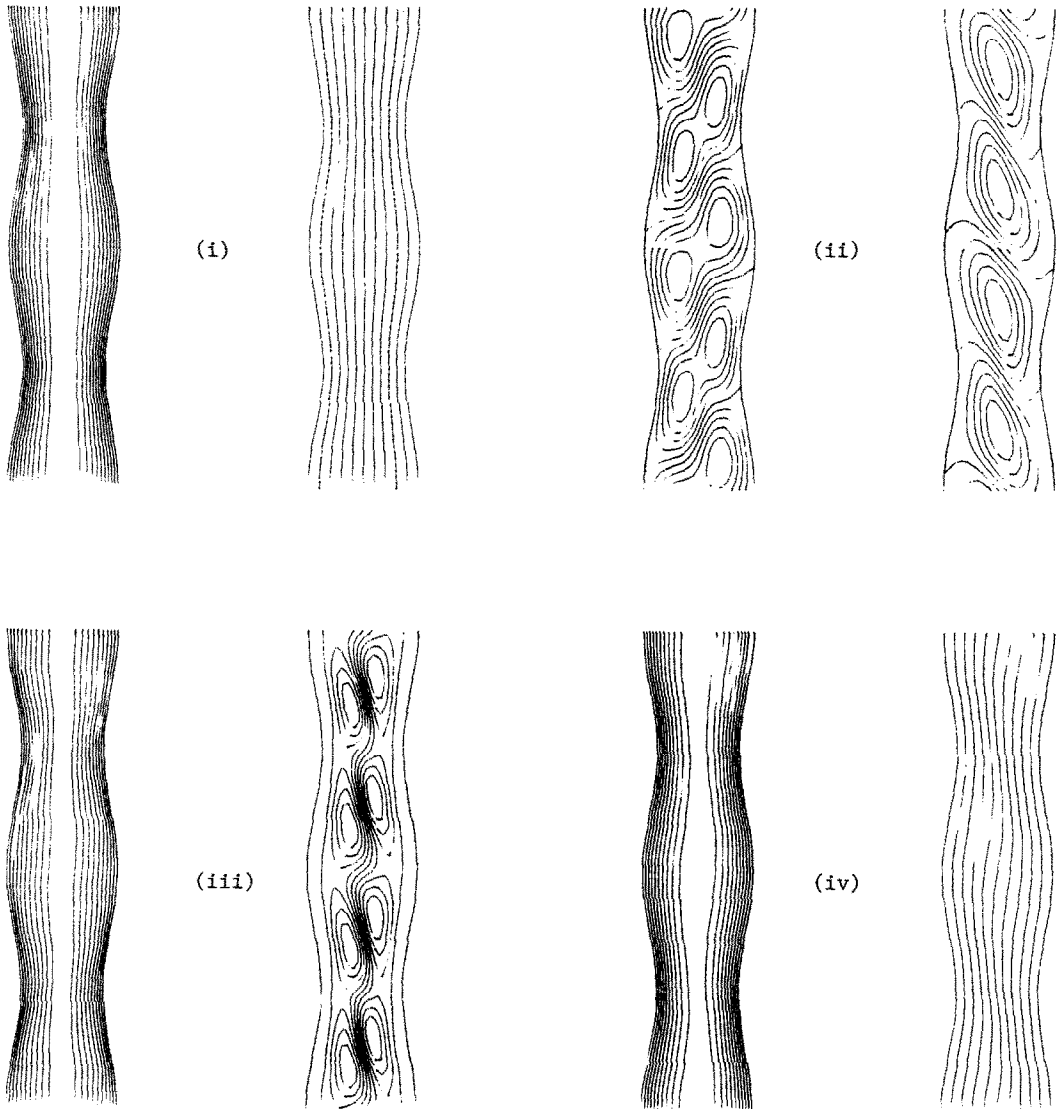


FIG. 2(c). The streamlines (left) and isotherms (right) when $\delta = 0.15$, $a_r = a_l = 1.0$ and $k = 1.5$: (i) $O(1)$, (ii) $O(\delta)$, (iii) $O(\delta^2)$, and (iv) resultant to $O(\delta^2)$. $Q = 0$, $A = 50$, $\beta = 0$.

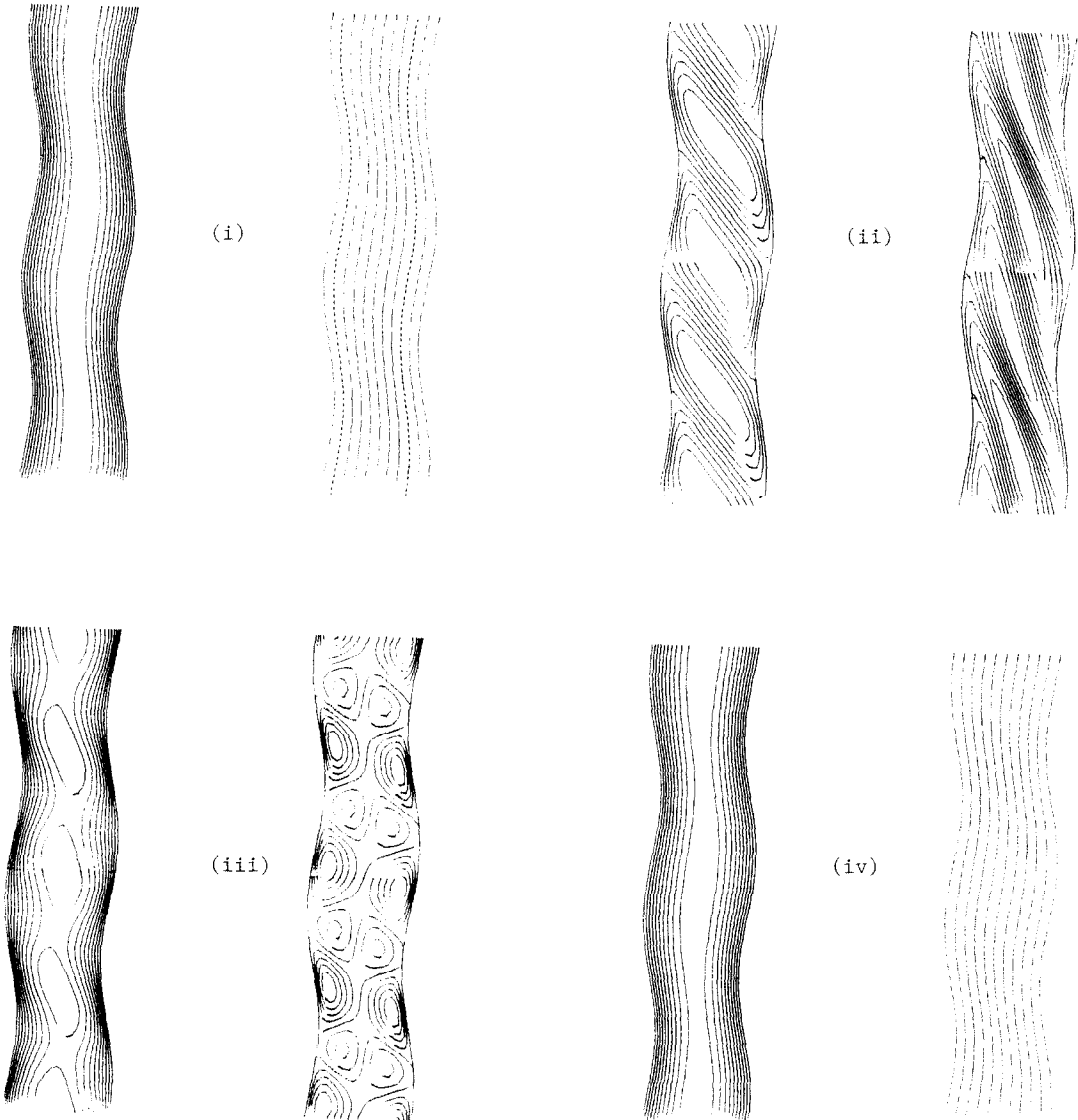


FIG. 2(d). The streamlines (left) and isotherms (right) when $\delta = 0.15$, $a_r = a_l = 1.0$ and $k = 1.5$: (i) $O(1)$, (ii) $O(\delta)$, (iii) $O(\delta^2)$, and (iv) resultant to $O(\delta^2)$. $Q = 0$, $A = 20$, $\beta = \pi/4$.

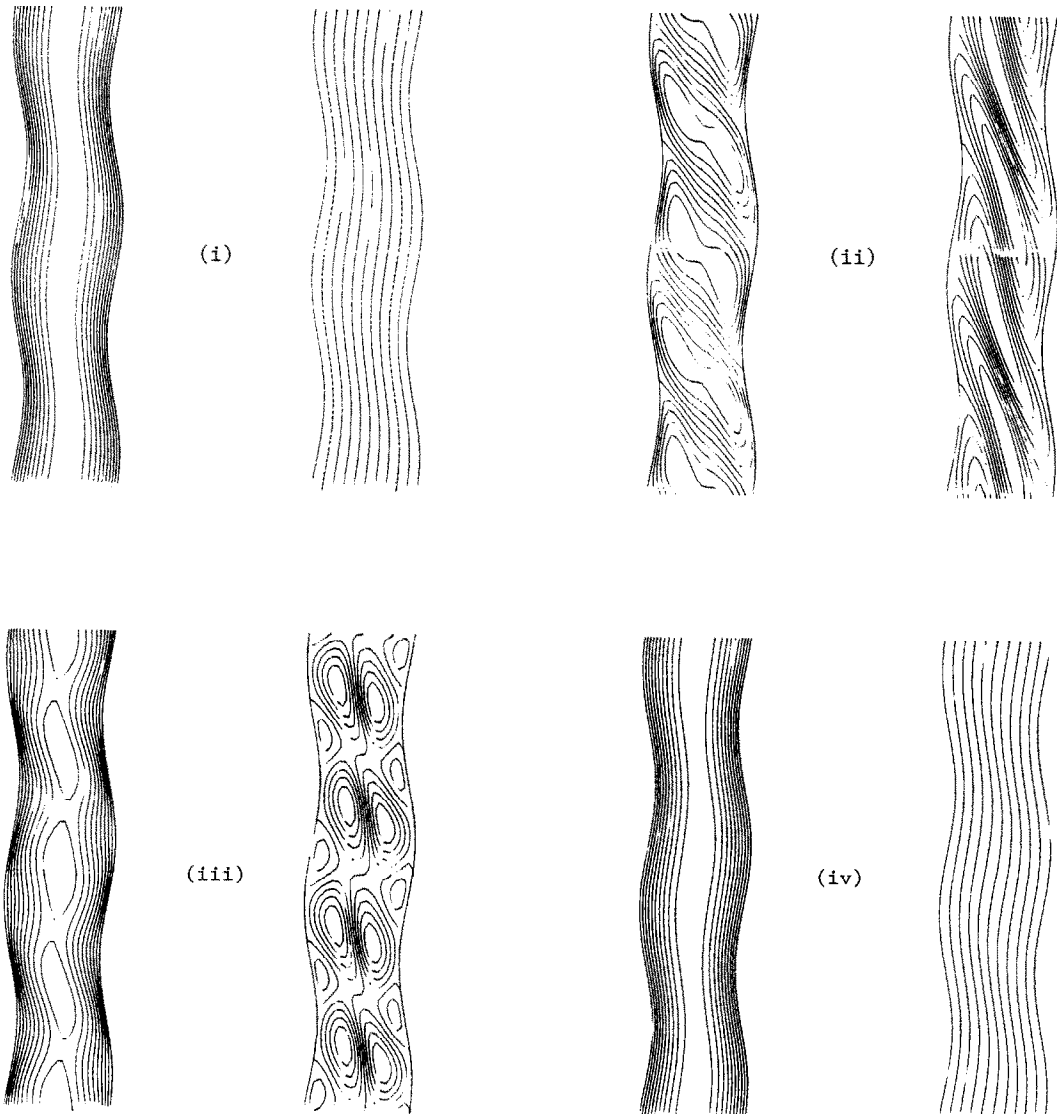


FIG. 2(e). The streamlines (left) and isotherms (right) when $\delta = 0.15$, $a_r = a_l = 1.0$ and $k = 1.5$: (i) $O(1)$, (ii) $O(\delta)$, (iii) $O(\delta^2)$, and (iv) resultant to $O(\delta^2)$. $Q = 0$, $A = 50$, $\beta = \pi/4$.

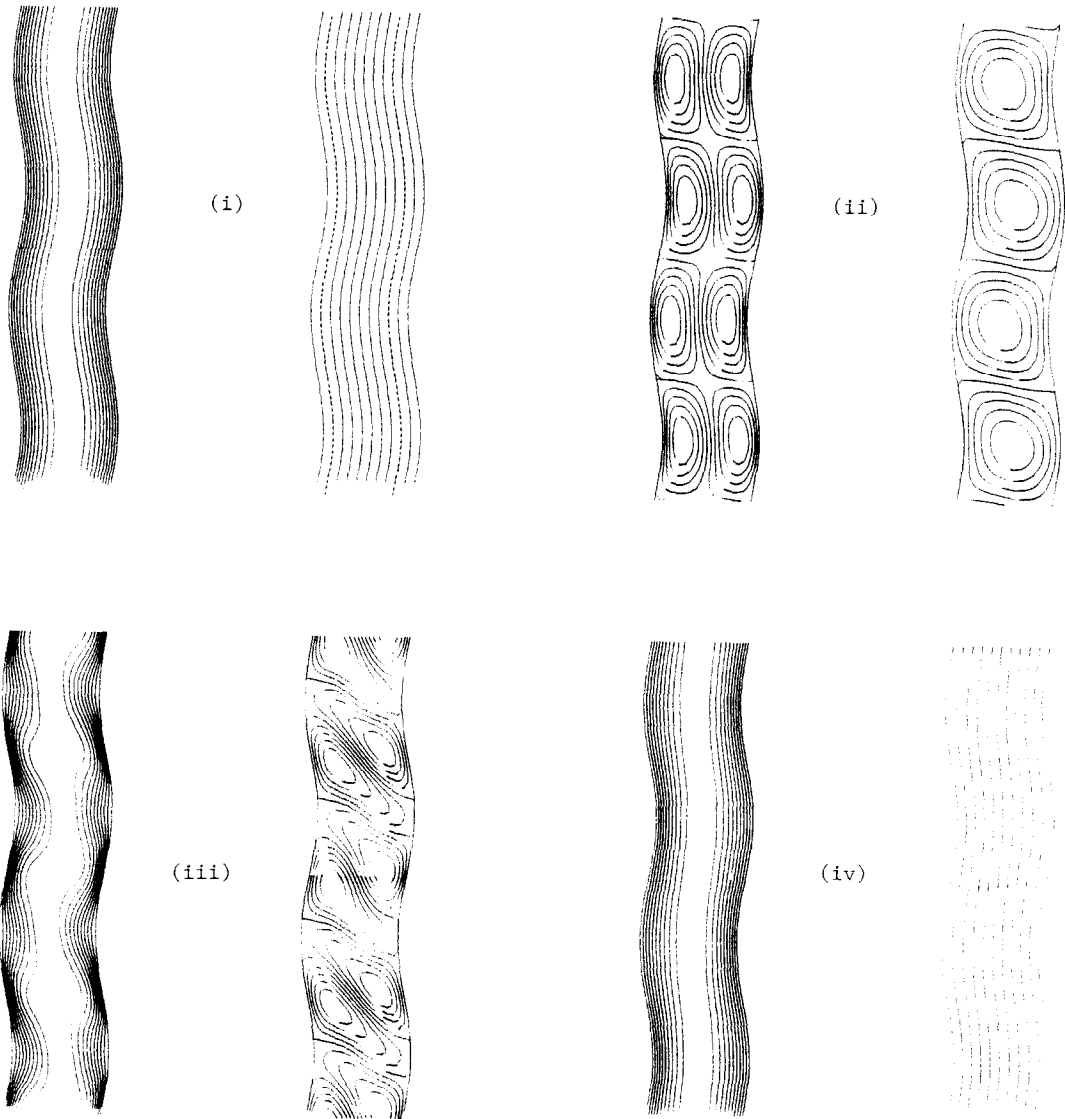


FIG. 2(f). The streamlines (left) and isotherms (right) when $\delta = 0.15$, $a_r = a_l = 1.0$ and $k = 1.5$: (i) $O(1)$, (ii) $O(\delta)$, (iii) $O(\delta^2)$, and (iv) resultant to $O(\delta^2)$. $Q = 0$, $A = 20$, $\beta = \pi/2$.

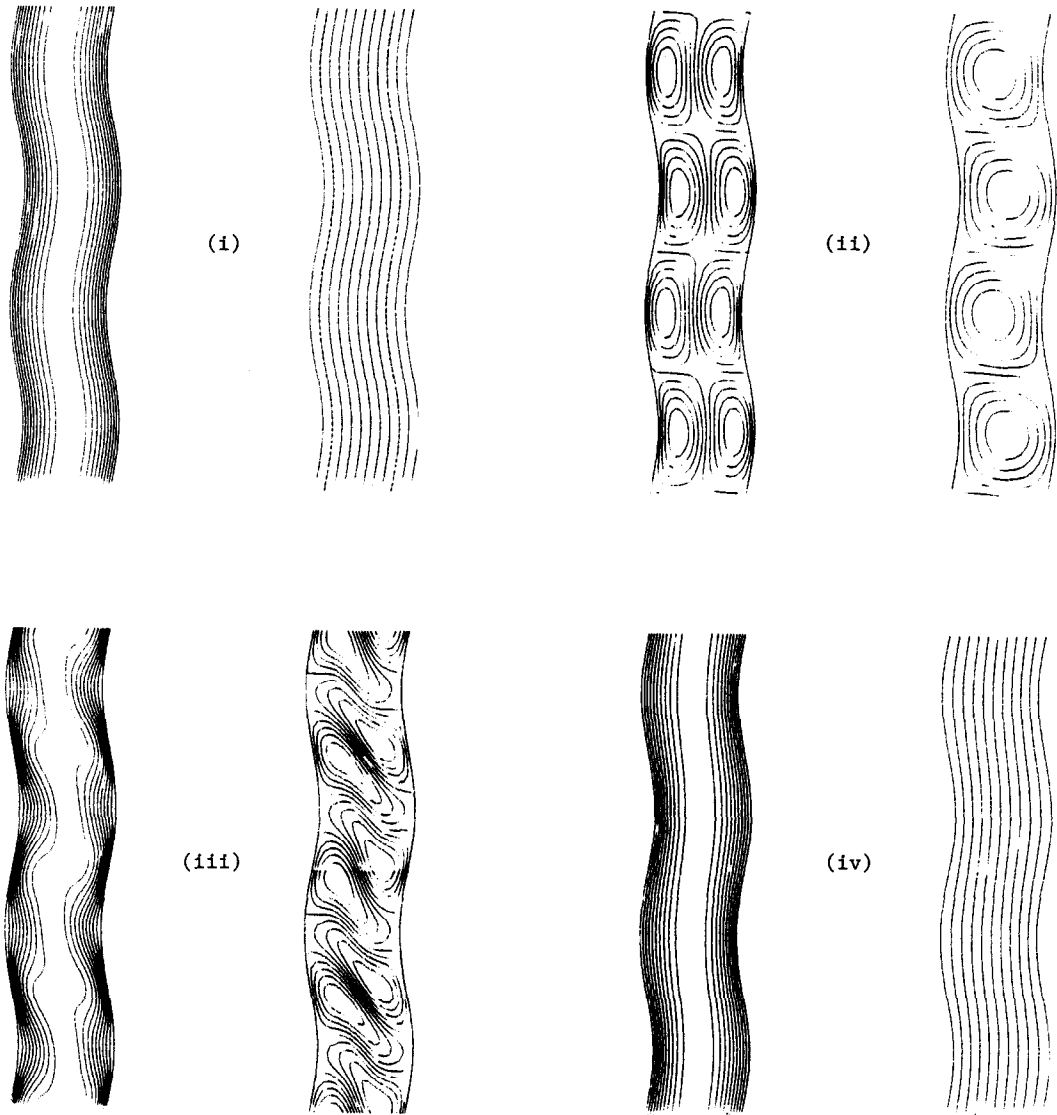


FIG. 2(g). The streamlines (left) and isotherms (right) when $\delta = 0.15$, $a_r = a_l = 1.0$ and $k = 1.5$: (i) $O(1)$, (ii) $O(\delta)$, (iii) $O(\delta^2)$, and (iv) resultant to $O(\delta^2)$. $Q = 0$, $A = 50$, $\beta = \pi/2$.

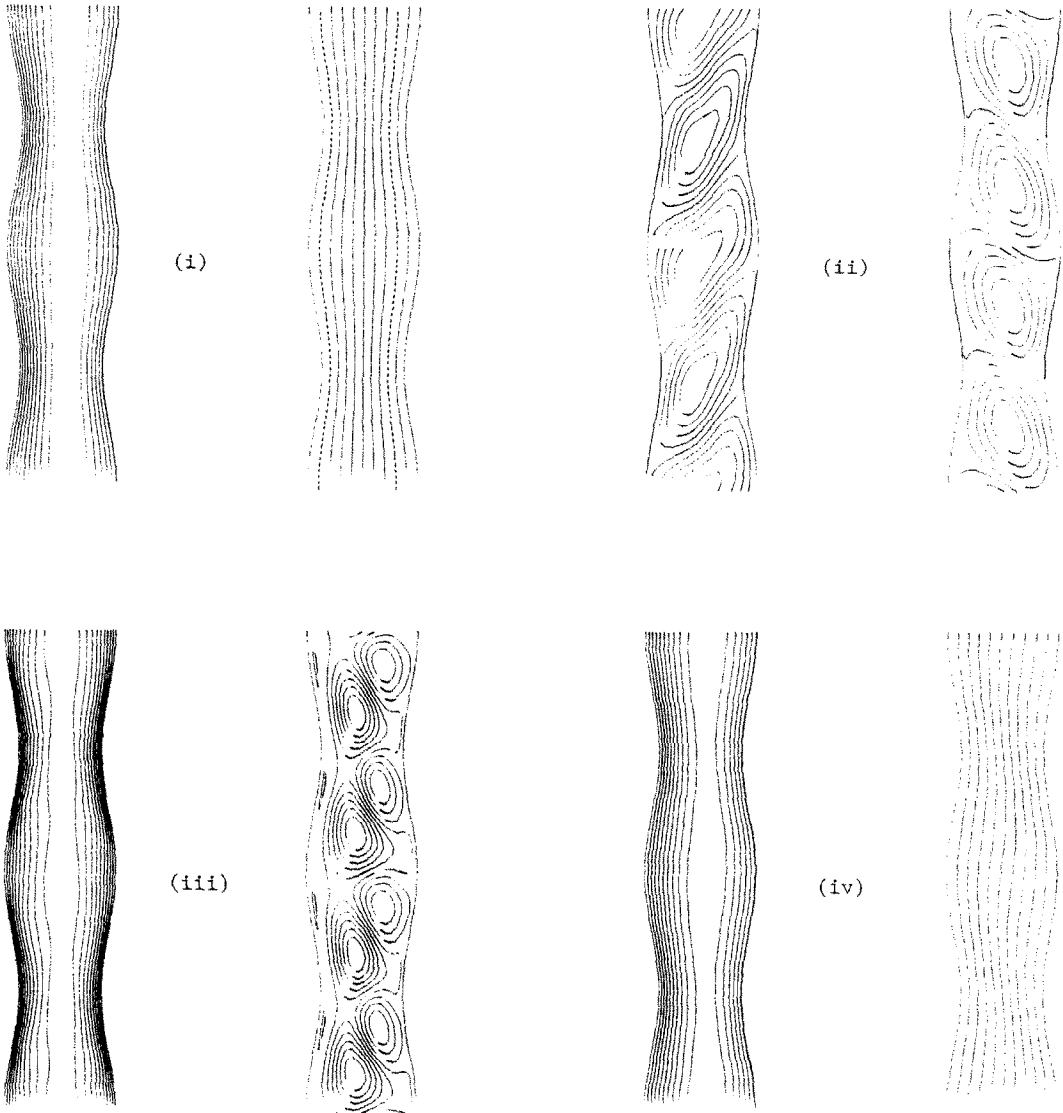


FIG. 2(h). The streamlines (left) and isotherms (right) when $\delta = 0.15$, $a_r = a_l = 1.0$ and $k = 1.5$: (i) $O(1)$, (ii) $O(\delta)$, (iii) $O(\delta^2)$, and (iv) resultant to $O(\delta^2)$. $Q = 5$, $A = 20$, $\beta = 0$.

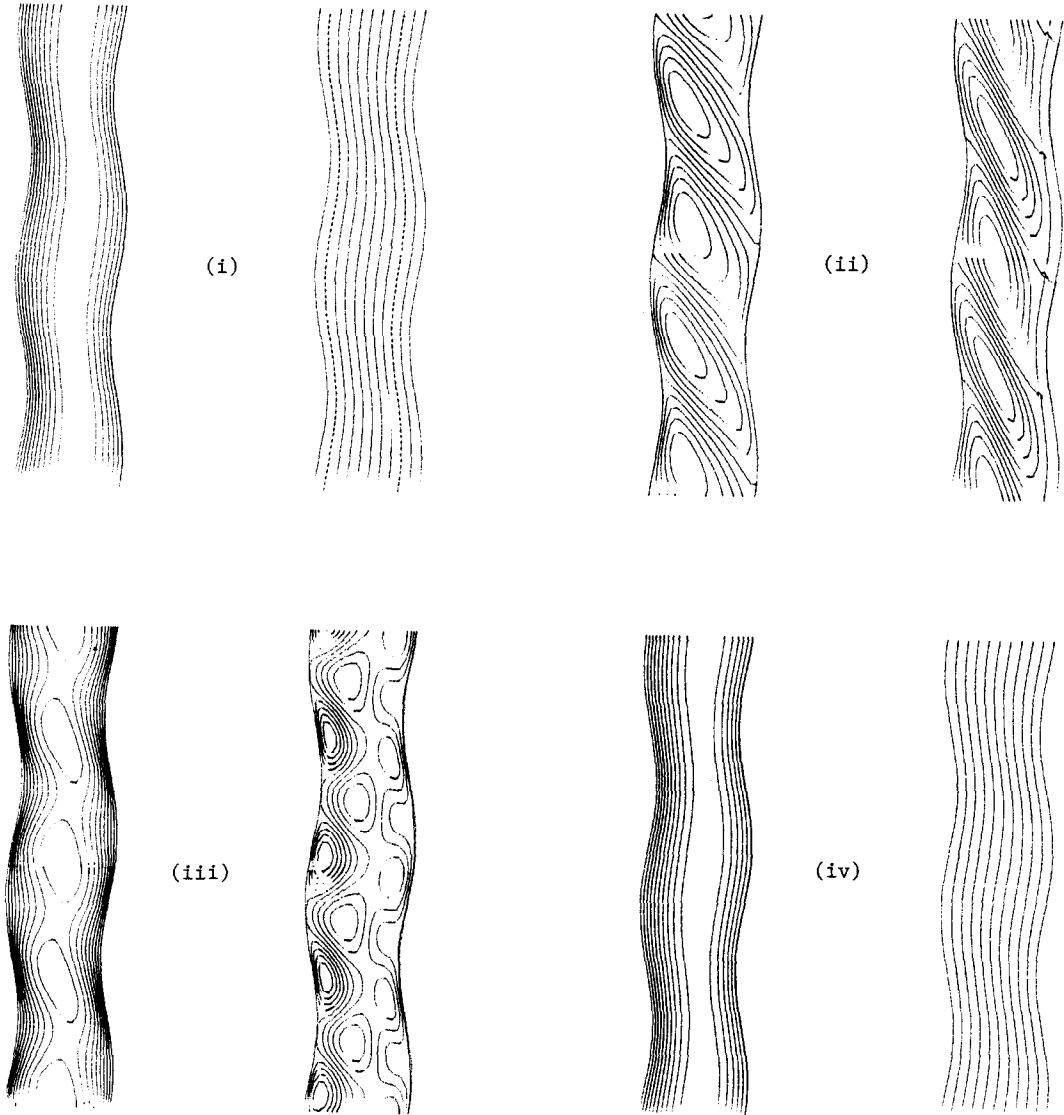


FIG. 2(j). The streamlines (left) and isotherms (right) when $\delta = 0.15$, $a_r = a_l = 1.0$ and $k = 1.5$: (i) $O(1)$, (ii) $O(\delta)$, (iii) $O(\delta^2)$, and (iv) resultant to $O(\delta^2)$. $Q = 5$, $A = 20$, $\beta = \pi/4$.

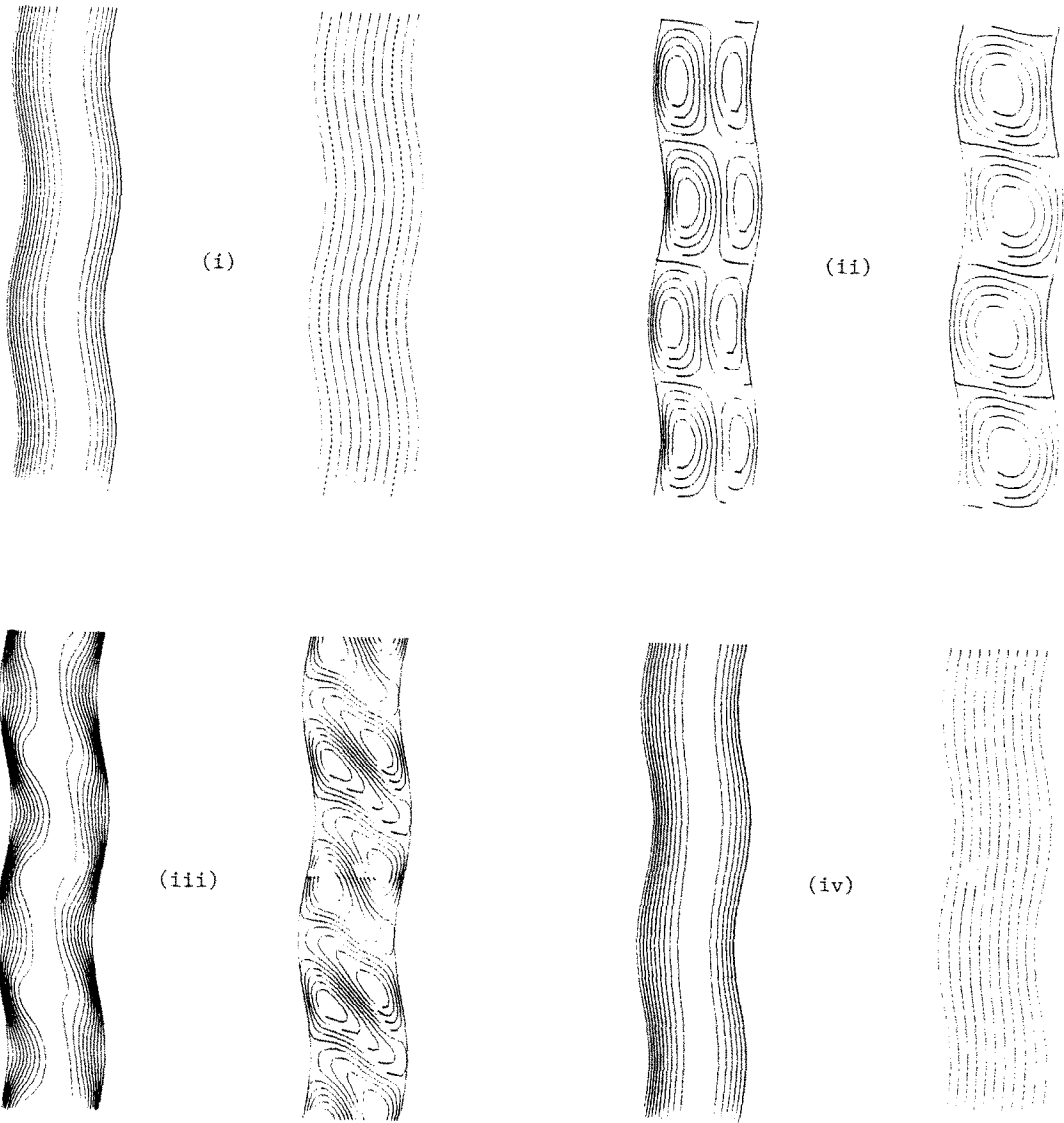


FIG. 2(k). The streamlines (left) and isotherms (right) when $\delta = 0.15$, $a_r = a_l = 1.0$ and $k = 1.5$: (i) $O(1)$, (ii) $O(\delta)$, (iii) $O(\delta^2)$, and (iv) resultant to $O(\delta^2)$. $Q = 5$, $A = 20$, $\beta = \pi/2$.

and the isotherms become more distorted due to the stronger secondary motions.

In Figs. 2(d) and (e) the corresponding results are shown for a configuration with a phase difference $\beta = \pi/4$ when $A = 20$ and 30 , respectively. Interesting qualitative changes are seen in the pictures for the different Rayleigh numbers: the $O(\delta)$ streamlines again display the tendency to pinch and split as A increases. In the sinuous configuration ($\beta = \pi/2$), Figs. 2(f) and (g), one can see that, compared with the varicose configuration, there is less vertical, but more horizontal distortion.

The effect of a weak vertical through-flow ($Q = 5$) on these three configurations when $A = 20$ is illustrated in Figs. 2(h)–(k). One can see that the vertical flow causes an asymmetry in the base- and secondary-flow patterns.

From a practical point of view, it is not the interesting changes in the flow and temperature fields that are significant, but rather the consequential changes in the heat-transfer characteristics. In Fig. 3 the Nusselt number for the varicose and sinuous configurations is compared. Clearly it is the out-of-phase (varicose) configuration that has a significantly higher heat transfer coefficient than other general configurations (the Nusselt numbers of which will lie between the values for these two extreme cases).

When $A = 0$, the Nusselt number is, in general, not equal to unity since the number represents the dimensionless heat transfer across a wavy slot. A little algebra shows that in this case

$$\overline{Nu} = 1 + \frac{\delta^2 k}{2 \sinh 2k} (\cosh 2k + \cos 2\beta)$$

to $O(\delta^2)$; these values are shown on Fig. 3 for the varicose ($\beta = 0$) and sinuous ($\beta = \pi/2$) cases when $k = 1.5$.

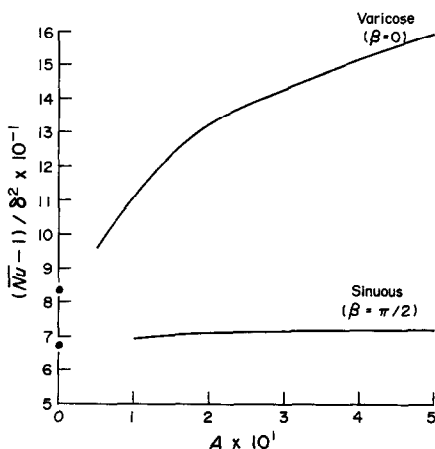


FIG. 3. Comparison of the calculated heat transfer characteristics of the varicose and sinuous configurations. The corresponding analytic results for $A = 0$ are denoted by ●.

CONCLUSIONS

A study has been carried out on the conduction regime in a porous vertical slot. The effects of spatially periodic variations on the flow have been considered and it has been shown that 'varicose' imperfections enhance the heat transfer significantly, compared with sinuous (or in-phase) imperfections.

REFERENCES

1. A. E. Gill, A proof that convection in a porous vertical slab is stable, *J. Fluid Mech.* **35**, 545–547 (1969).
2. S. Klarsfeld, Champs de température associés aux mouvements de convection naturelle dans un milieu poreux limité, *Rev. Gén. Thermique* **9**, 1403–1423 (1970).
3. M. P. Vlasuk, Heat transfer with natural convection in permeable porous media, *Proc. IVth All-Union Heat and Mass Transfer Conf.*, Minsk (1972).
4. P. H. Holst and K. Aziz, A theoretical and experimental study of natural convection in a confined porous medium, *Can. J. Chem. Engng* **50**, 232–241 (1972).
5. S. A. Bories and M. A. Combarous, Natural convection in a sloping porous layer, *J. Fluid Mech.* **57**, 63–79 (1973).
6. C. G. Bankvall, Natural convection in a vertical permeable space, *Wärme- und Stoffübertr.* **7**, 22–30 (1974).
7. J. E. Weber, The boundary-layer régime for convection in a vertical porous layer, *Int. J. Heat Mass Transfer* **18**, 569–573 (1975).
8. P. J. Burns, L. C. Chow and C. L. Tien, Convection in a vertical slot filled with porous insulation, *Int. J. Heat Mass Transfer* **20**, 919–926 (1977).
9. K. L. Walker and G. M. Homsy, Convection in a porous cavity, *J. Fluid Mech.* **87**, 449–474 (1978).
10. A. Bejan and C. L. Tien, Natural convection in a horizontal porous medium subjected to an end-to-end temperature difference, *Trans. Am. Soc. Mech. Engrs, Series C, J. Heat Transfer* **100**, 191–198 (1978).
11. N. Seki, S. Fukusako and J. Inaba, Heat transfer in a confined rectangular cavity packed with porous media, *Int. J. Heat Mass Transfer* **21**, 985–989 (1978).
12. A. Bejan, On the boundary layer régime in a vertical enclosure filled with a porous medium, *Lett. Heat Mass Transfer* **6**, 93–102 (1979).
13. P. G. Simpkins and P. A. Blythe, Convection in a porous layer, *Int. J. Heat Mass Transfer* **23**, 881–887 (1980).
14. C. E. Hickox and D. K. Gartling, A numerical study of natural convection in a horizontal porous layer subjected to an end-to-end temperature difference, *Trans. Am. Soc. Mech. Engrs, Series C, J. Heat Transfer* **103**, 797–802 (1981).
15. P. A. Blythe, P. G. Daniels and P. G. Simpkins, Thermally driven cavity flows in porous media. I. The vertical boundary layer structure near the corners, *Proc. R. Soc.* **A380**, 119–136 (1982).
16. P. G. Daniels, P. A. Blythe and P. G. Simpkins, Thermally driven cavity flows in porous media. II. The horizontal boundary layer structure, *Proc. R. Soc.* **A382**, 135–154 (1982).
17. P. A. Blythe, P. G. Simpkins and P. G. Daniels, Thermal convection in a cavity filled with a porous medium: a classification of limiting behaviours, *Int. J. Heat Mass Transfer* **26**, 701–708 (1983).
18. V. Prasad and F. A. Kulacki, Convective heat transfer in a rectangular porous cavity—effect of aspect ratio on flow structure and heat transfer, *Trans. Am. Soc. Mech. Engrs, Series C, J. Heat Transfer* **106**, 158–165 (1984).
19. P. G. Daniels, P. A. Blythe and P. G. Simpkins, Thermally driven shallow cavity flows in porous media: the intermediate régime, *Proc. R. Soc.* **406**, 263–285 (1986).
20. P. G. Daniels, Transition to the convective régime in a

- vertical slot, *Int. J. Heat Mass Transfer* **28**, 2071–2077 (1985).
21. P. G. Daniels, Convection in a vertical slot, *J. Fluid Mech.* **176**, 419–441 (1987).
22. M. C. Wynne, The effect of boundary imperfections on free convection in fluid layers, Ph.D. Thesis, University of Bristol (1987).

CONVECTION THERMIQUE PERMANENTE ET BIDIMENSIONNELLE
DANS UNE COUCHE POREUSE VERTICALE AVEC DES IMPERFECTIONS
SPATIALEMENT PERIODIQUES AUX FRONTIERES

Résumé—Une convection thermique permanente et bidimensionnelle, dans une fente verticale, remplie d'un milieu poreux saturé, est considérée avec des parois latérales maintenues à des températures différentes constantes et non parallèles, par exemple avec des ondulations de surface. Les non-uniformités spatiales sur les deux parois sont supposées avoir de faibles amplitudes et des nombres d'onde communs (arbitraires). L'attention est portée sur l'écoulement au coeur, qui est supposé être situé dans le régime conductif. En l'absence des non-uniformités cet écoulement est inconditionnellement stable, en conséquence l'écoulement est purement baroclinique et il n'y a pas d'instabilité thermoconvective. On présente les résultats en nombre de Nusselt et on trouve qu'il n'y a pas d'accroissement sensible du transfert de chaleur.

STATIONÄRE ZWEIDIMENSIONALE THERMISCHE KONVEKTION IN EINEM
SENKRECHTEN SPALT MIT ÜBERFLUTETER SCHÜTTUNG UND UNREGELMÄSSIGEN
WÄNDEN

Zusammenfassung—Die stationäre, zweidimensionale thermische Konvektion in einem senkrechten Spalt, der mit einer überfluteten Schüttung gefüllt ist, wird betrachtet. Die Wände werden auf konstanten, jedoch unterschiedlichen Temperaturen gehalten und sind nur ungenügend parallel ausgerichtet, d. h. an der Oberfläche wellig. Die Amplitude der Wellen ist klein, ihre Wellenzahl beliebig. Besonderes Augenmerk wird auf die Kernströmung gerichtet, von der angenommen wird, daß sie im Bereich der Wärmeleitung liegt. Ohne Unebenheiten ist diese Strömung immer stabil, das heißt, es liegt eine Strömung ohne konvektionsbedingte Instabilitäten vor. Es werden *Nu*-Zahlen dargestellt, und es wird gezeigt, daß eine Phasenverschiebung bei der Welligkeit den Wärmeübergang erheblich verbessert.

СТАЦИОНАРНАЯ ДВУХМЕРНАЯ ТЕПЛОВАЯ КОНВЕКЦИЯ В ВЕРТИКАЛЬНОЙ
ПРИСТОЙ ЩЕЛИ С ПРОСТРАНСТВЕННЫМИ ПЕРИОДИЧЕСКИМИ ДЕФЕКТАМИ
ГРАНИЦ

Аннотация—Рассматривается стационарная двухмерная тепловая конвекция в вертикальной щели, заполненной насыщенной пористой средой. Боковые стенки имеют различную постоянную температуру и неровную поверхность. Предполагается, что пространственные неоднородности обеих стенок имеют малые амплитуды и общее (произвольное) волновое число. Особое внимание уделено ядру потока, для которого предполагается кондуктивный режим. При отсутствии неоднородностей этот поток, безусловно, стабилен, соответственно реальный поток является чисто бароклинным и не характеризуется теплоконвективной неустойчивостью. Представлены результаты числа Нуссельта и найдено, что сдвинутые по фазе дефекты значительно усиливают теплоперенос.